This article has been accepted for publication in a future issue of this journal, but has not been fully edited. Content may change prior to final publication. Citation information: DOI 10.1109/TASC.2016.2539148, IEEE Transactions on Applied Superconductivity

Fast ramped Quadrupoles for the Transition Jump Scheme of the SIS100 Synchrotron of the FAIR Project

Hanno Leibrock, Jan Patrick Meier, Carsten Mühle, Henning Raach, Peter Rottländer, Seong Yeub Shim, and Stefan Wilfert, *GSI*

***Abstract*—A gamma transition jump scheme has been developed for the heavy ion synchrotron SIS100 to modify the gamma transition during the acceleration of protons in such a way that the speed at which the relativistic gamma of the beam crosses the transition gamma is increased by two orders of magnitude. The transition crossing will be at gamma = 8.9 which corresponds to a kinetic proton energy of 7.4 GeV and a beam rigidity of about 28 Tm. The scheme employs fast ramped quadrupoles with a ramping time of 0.5 milliseconds from the maximum integral gradient of 0.4 Tesla to the minimum integral gradient of minus 0.4 Tesla. Each of the 12 fast ramped quadrupoles is embedded inside the cryostats of the so called quadrupole doublet modules together with two main superconducting quadrupoles and one corrector magnet. The vacuum chamber, coils and iron yoke are cooled with liquid helium. Nevertheless the coils are made of standard copper tubes with a residual resistivity ratio of approximately 100 to avoid quench problems due to the fast ramping.**

The requirements and design of these normal conducting magnets inside the cryogenic environment are described.

***Index Terms*—Accelerator magnets, fast ramped magnets, gamma transition.**

I. Introduction

Experiments with antiprotons are one of the main topics of the Facility for Antiproton and Ion Research (FAIR) [1]. Antiprotons will be produced with a pbar-target with protons of energies up to 29 GeV. For an effective production rate of antiprotons, the primary protons are accelerated up to a relativistic γ of 32 in the SIS100 synchrotron. Proton acceleration without gamma transition, the point where a relative momentum error $\Delta p/p$ does not lead to a relative change in the revolution frequency $\Delta f/f = 0$ [2], is not possible with the SIS100 and a transition shift scheme is not feasible. Therefore a transition jump scheme has been implemented with a γ_t of 8.9. The change of γ_t is realized with a quick modification of the dispersion in the arcs of the SIS100 that will be done with the fast ramped so called γ_t-jump quadrupoles. The frame conditions, design principles and solutions of these quadrupoles inside the unusual cold environment for normal conducting magnets will be presented.

H. Leibrock, J. P. Meier, C. Mühle H. Raach P. Rottländer, S. Y. Shim, and S. Wilfert are with the GSI Helmholtzzentrum für Schwerionenforschung GmbH, Planckstraße 1, D-64291 Darmstadt, Germany (h.leibrock@gsi.de)

II. Requirements

A. Parameters

The chosen transition jump scheme requires one pair of fast pulsed quadrupoles per sector. The two quadrupoles of a pair need to be operated synchronously with fields of equal magnitude but opposite sign. The six pairs, one for each sector, also have to be synchronized precisely. During a single cycle, the field in the quadrupoles must reverse its sign, which means the power converters need to be bipolar.

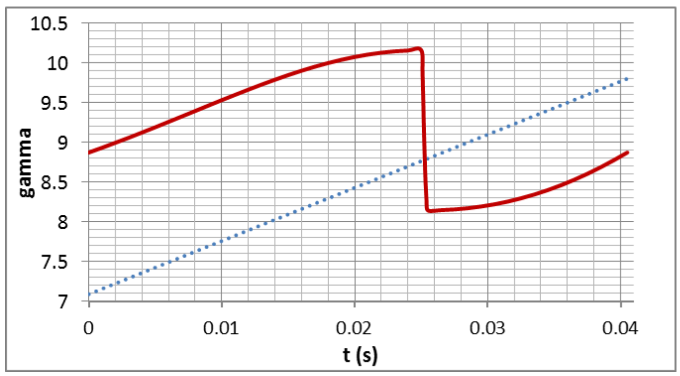

Figure 1: Time evolution of γ_t during the jump (red line), compared to the evolution of the beam γ (dotted blue line).

The strength of the jump quadrupoles is determined by the required change in γ_t which is approximately $\Delta\gamma_t = 2$. This total change is composed of a positive shift of $\Delta_+\gamma_t = 1.3$ and a negative shift of $\Delta_-\gamma_t = -0.7$ (Figure 1). These shifts are produced by integral jump quadrupole strengths from about +0.4 T to -0.4 T. The main parameters of the γ_t-jump quadrupoles are listed in Table I.

TABLE I
PARAMETERS OF THE γ_T-JUMP QUADRUPOLES

Parameter	Value
Number of magnets	12
Max. integral gradient	0.4 T
Min. integral gradient	-0.4 T
Max. gradient	1 T/m
Overall magnet length (with coil)	470 mm
Yoke length	361 mm
Yoke width	260 mm
Yoke height	260 mm

1051-8223 (c) 2015 IEEE. Personal use is permitted, but republication/redistribution requires IEEE permission. See http://www.ieee.org/publications_standards/publications/rights/index.html for more information.

Integral field quality inside Reference radius ΔB/B	1 %
Reference radius	30 mm
Rise time from zero to max	25 ms
Jump time from max to min	0.5 ms
Fall time from min to zero	15 ms
Maximum current (both directions)	±200 A
Maximum stored energy	6.6 J
Inductance	0.33 mH
Maximum inductive voltage	264 V
Maximum ramp rate	1600 T/s
Maximum repetition rate	0.5 Hz

For power converters, the voltage in the table would have to be doubled because two γ_t-jump quadrupoles are powered in series.

B. *Frame conditions*

Most magnets of the SIS100 synchrotron are superferric magnets with helium cooled coils, cold yokes and actively cooled beam vacuum chambers. The configuration with cryogenically cooled vacuum chambers enables the generation and maintaining of UHV or even XHV pressures by means of cryopumping. Typically, the main quadrupole magnets are combined into doublets which are assembled together with two corrector magnets inside one common cryostat [3]. One γ_t-jump quadrupole can be installed instead of such a corrector magnet.

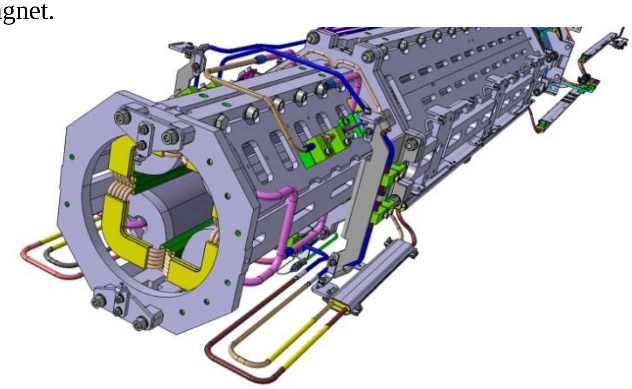

Figure 2: Model of a γ_t-jump quadrupole inside its frame which is installed on one end of a main quadrupole. The two clamps at the front fix the common vacuum chamber.

All magnets are cooled with a forced two phase helium flow. The coils of the superconducting magnets are made of superconducting Nuclotron type cables [4]. The coils of the γ_t-jump quadrupole consist of copper tubes wrapped into two layers of adhesive Kapton foil. The helium first flows through the coil and then through pipes on the yoke. The yoke is embedded in a stainless steel frame, which holds the yoke, helium pipes, current leads, vacuum chamber and bus bars for the connection to the neighboring quadrupole doublets. This leads to the space restrictions listed in table 1. The inner shape of the yoke of a γ_t-jump quadrupole is exactly the same as for a main quadrupole to ensure enough space for the common vacuum chamber and a good field quality. After acceleration to a kinetic energy of 7.4 GeV per proton, the elliptic cross section of the beam is reduced from 120 mm × 60 mm to a circular beam size with 60 mm diameter. This reduction helps reaching the required field quality even if detrimental influences such as eddy currents or neighboring strong quadrupoles are working against this. Figure 3 shows the Opera 2d model of the quadrupole.

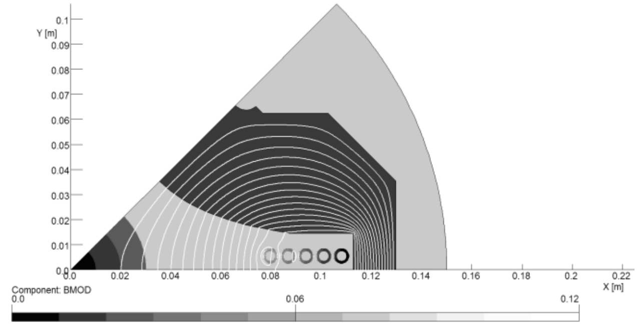

Figure 3: Opera 2D-model of the γ_t-jump quadrupole. Using all symmetries only 1/8 of the cross section must be simulated. The inscribed pole radius is 50 mm to ensure space for the vacuum chamber. The reference radius is only 30 mm. Flux lines and flux densities [T] inside the five turns of the coil and the required good field region represents the situation at the end of the jump from 200 A to -200 A.

III. Current Leads

For each magnet, two separate currents leads are necessary, consisting of copper with residual resistivity ratio between 7-10. The maximum current is set to 200 Ampere to keep heat introduction through the leads to the cold mass low. The current leads are divided into two parts. An upper warmer part leads from the warm terminal at 300 K to a thermal anchor of approximately 70 K. It is planned to have a length of about 250 mm and a cross section of $5mm^2$. The lower colder part is between the anchor and the magnet. Its proposed length is about 1320 mm and the cross section 20 mm^2. The leads are also wrapped with Kapton. During operation as described in Table I, an average heat input of 1.8 W per current lead into the anchor and 0.8 W per current lead into the cold mass is expected. In case the SIS100 accelerates particles other than protons, the γ_t-jump quadrupoles are not powered and the heat input is 0.18 W into the anchor and 0.35 W into the cold mass.

IV. Coil

The coil consists of 5 turns in one layer to achieve a maximum gradient of 1 T/m with 200 A.

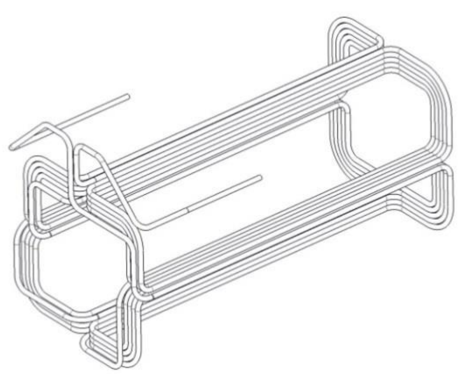

Figure 4: Coil for all four poles of one γ_t-jump quadrupole

One single copper tube piece with a residual resistivity ratio of approximately 100 will be used to wind the coils for all four poles of one quadrupole to avoid fault-prone connections (see Figure 4). The resistance of the coil at 4 K is about 0.2 mΩ.

1051-8223 (c) 2015 IEEE. Personal use is permitted, but republication/redistribution requires IEEE permission. See http://www.ieee.org/publications_standards/publications/rights/index.html for more information.

This article has been accepted for publication in a future issue of this journal, but has not been fully edited. Content may change prior to final publication. Citation information: DOI 10.1109/TASC.2016.2539148, IEEE Transactions on Applied Superconductivity

The outer diameter is 6 mm with a wall thickness of 1 mm. Glass fibre reinforced plastic pieces position the turns inside and outside the yoke to prevent coil moving. Two ceramic voltage breakers electrically separate cooling tubes from the coil.

V. Cross talk between main and jump quadrupole

The distance between the yokes of the main and gamma quadrupole is only 203 mm. Therefore, the mutual influence of the magnets had to be investigated. Table II shows integral quadrupole fields of both magnets at R_{ref} = 30 mm for different field levels. The gradient of the main quadrupoles at γ_t jump is 3.5 T/m. As a result, the magnets work independently without significant cross talk. The integrals of both powered magnets are the sum of single powered magnets.

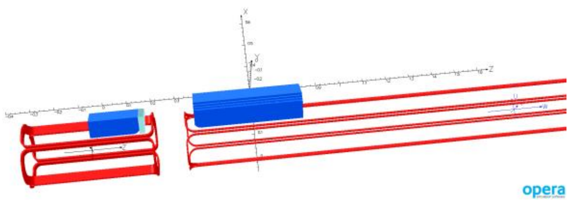

Figure 5: Opera 3d-model of the γ_t-jump quadrupole (left) with the main standard quadrupole (right). To examine the cross talk between these magnets, only a small part of the main quadrupole and a half of the γ_t-jump quadrupole was simulated. In addition all symmetries were used to reduce computing time.

TABLE II
FIELD INTEGRALS AT R_{REF} = 30 MM

γ_t-jump	Main	Simulated integral	Expected integral
100 %	Off	0.00606950	
0	On	0.08949261	
50%	On	0.09252734	0.09252736
100%	On	0.09556208	0.09556211
-100%	On	0.08342306	0.08342311

The expected integral is the sum of the simulated integral of the main quadrupole plus the simulated integral of the γ_t-jump quadrupole times the factors 0.5,1, and -1. The numerous decimal places are only shown to demonstrate that the sum is not exactly the same and the integrals are results of different simulations.

VI. Eddy currents

The fast ramping, and even more the sudden jump from maximum current to minus maximum current, induce eddy current effects which must be considered in design and operation.

A. Eddy currents in the vacuum chamber

The γ_t and the adjacent superconducting quadrupole magnet have a common beam vacuum chamber. Its wall thickness is only 0.3 mm to minimize eddy current. Ribs are welded onto the chamber for reinforcement. Figure 6 shows the used ANSYS model. Due to high material requirements on magnetic permeability, the common vacuum chamber is made of special stainless steel grade, P506 [5]. Cooling pipes are located on top, bottom and both lateral sides. The cooling pipes are electrically insulated from the chamber by a thin Al_2O_3 layer. Hence, eddy current effects in the cooling pipes can be neglected. Due to the small maximum field at the chamber, B = 300 ~ 500 Gauss, there is no noticeable exponential field decay. However, a small time delay can be found during jump process. It is about 22.4 μsec. The maximum current density at the outermost chamber sides is 15 A/mm^2.

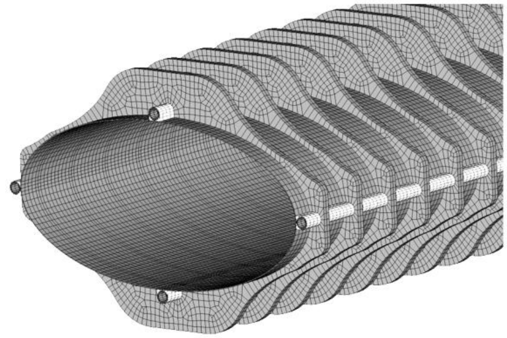

Figure 6: ANSYS model of the vacuum chamber for eddy current simulation induced by the jump. The temperature of the four cooling pipes is set to 4.5 K.

The time averaged power dissipation for one cycle is 0.536 W. The time dependent development of the hottest point on the vacuum chamber is shown in Figure 7. As the temperature does not exceed 7.5 K effective cryopumping is not impaired,

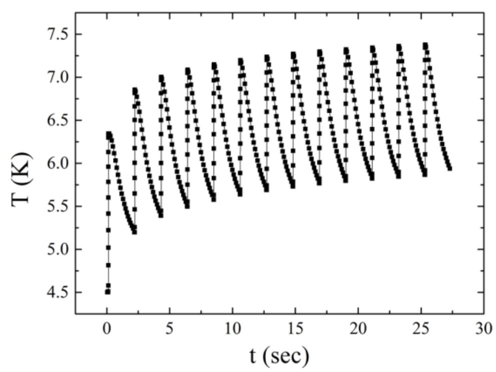

Figure 7: Maximum temperature on the chamber side in the first 13 cycles. The maximum steady state temperature is about 7.5 K.

B. Eddy currents in the yoke

For the thin laminations the density of power dissipation P_V in the lamination due to eddy currents may be expressed as [6]:

$$P_V = \frac{1}{6}\sigma B^2 a^2 \omega^2 \tag{1}$$

And for the yoke volume:

$$P = l \cdot \int_S P_v ds = \frac{l\sigma a^2 \omega^2}{6} \int_S B^2 ds \tag{2}$$

With a half-thickness of the lamination a = 0.175 mm, an effective pulsatance ω = 6.28 10^3/s, a conductivity σ = 2·10^6 Ohm^{-1}·m^{-1} (typical value of electrical steel at 4 K [6]), the yoke length l = 361 mm, and the field integration over the cross section of the magnet equal 2.4·10^{-4} T^{2}m^2 a power loss

1051-8223 (c) 2015 IEEE. Personal use is permitted, but republication/redistribution requires IEEE permission. See http://www.ieee.org/publications_standards/publications/rights/index.html for more information.

of 35 W during the jump is calculated. The longest time constant of the laminated structure may be estimated as [6]:

$$\tau = \frac{4a^2\mu\sigma}{\pi^2} \tag{3}$$

In this unsaturated case with $\mu \approx 2000\cdot\mu_0$, τ is about 0.06 ms. The eddy currents in 0.35 mm thick laminations vanish immediately.

Two additional components must be considered: The eddy currents inside laminations due to magnetic flux components perpendicular to the laminations at the ends of the iron yoke and eddy currents inside the end plates made of stainless steel. These end plates are necessary to prevent the laminations at the end from splitting. Unfortunately these plates cannot be easily replaced by other materials like glass fibre reinforced plastic because of the shrinking during cooling of the different parts of the quadrupole and the resulting stresses. These losses are calculated with Opera 3d simulations using the γ_t-jump quadrupole model shown on the left side of Figure 5. Figure 8 presents the results of these simulations.

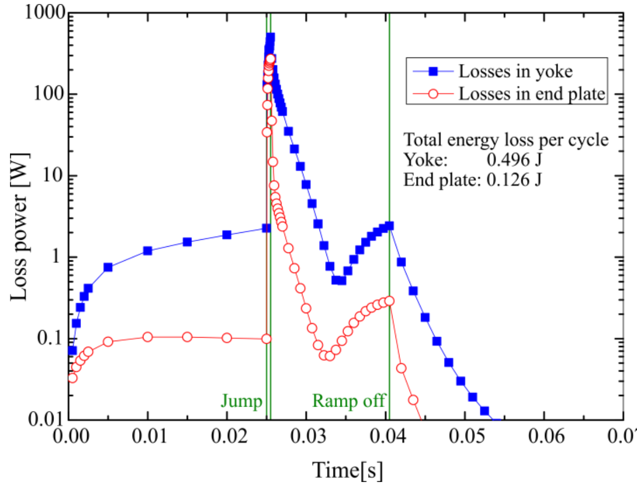

Figure 8: Eddy current losses inside the stainless steel end plates and the laminations. In this simulation the thickness of the laminations is infinitesimal. Only the magnetic flux components perpendicular to the laminations induce eddy currents.

C. *Eddy currents in the coil*

A transient opera 2d simulation has been done to estimate the contribution of eddy currents in the coil, based on the model of Figure 3. The overall current in each turn is set to 200 A. The average current density is 12.7 A/mm^2, but due to the eddy currents, local current densities exceeding 1000 A/mm^2 in both directions will be reached. The results are presented in Figure 9 and Table III. The average power dissipation is 0.86 W per magnet.

TABLE III
ENERGY DISSIPATION IN EACH TURN FOR ONE CYCLE

Turn	1	2	3	4	5
Average flux at turn (mT)	72.6	59.2	43.6	26.9	11.2
Energy dissipation (J/m)	0.256	0.191	0.107	0.044	0.006

The energy dissipation due to eddy currents inside the conductor is highest in the innermost turn 1.

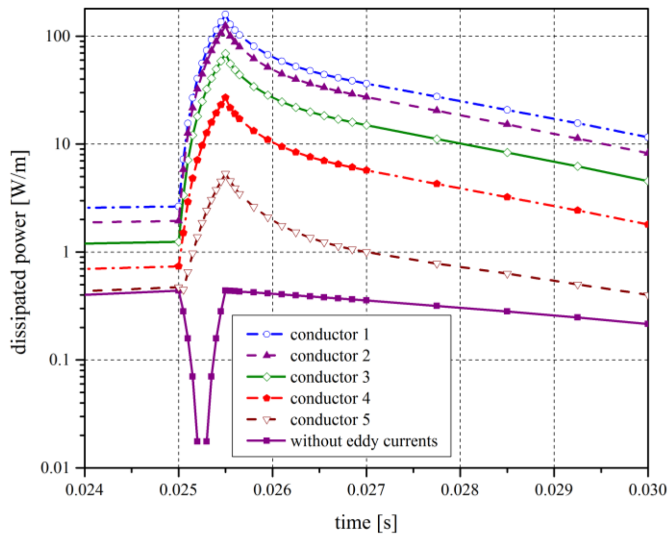

Figure 9: The energy dissipation due to eddy currents inside the conductor during and after the jump.

VII. Expected Heat Introduction into the Cold Mass

All mentioned sources of heat introduction to the cold mass are summarized in Table IV. The expected average heat introduction to the cold mass is 4.14 W. This is well below the acceptable limit of 10 W. Possible optimizations would lead only to small changes of the overall heat introduction. Therefore the prototype of the γ_t-jump quadrupole will be manufactured as described.

TABLE IV
SOURCES OF HEAT INTRODUCTION TO COLD MASS

Source	Value
Radiation to cold mass	0.5 W
Current leads not powered	0.7 W
Current leads operating in γ_t-jump quadrupole cycle	1.6 W
Eddy currents of vacuum chamber	0.54 W
Eddy currents of yoke transverse to laminations	0.01 W
Eddy currents of yoke end parts	0.5 W
Eddy currents of both end plates	0.13 W
Eddy currents inside the conductor	0.86 W

All values are average values of a typical two seconds long cycle of proton acceleration with γ_t-jump.

VIII. Conclusion

Field quality requirements can be easily reached due to the relatively large distance between yoke and good field region. More critical is heat introduction due to current leads, eddy currents, ohmic losses and thermal radiation. Some compromises had to be found and made. The technical drawings are finished. Construction and testing of a γ_t-jump quadrupole prototype is in preparation. First test results are expected by end of 2016.

Acknowledgment

The authors want to thank Alexander Kalimov from the St. Petersburg State Polytechnic University for providing some of the FEM simulations.

1051-8223 (c) 2015 IEEE. Personal use is permitted, but republication/redistribution requires IEEE permission. See http://www.ieee.org/publications_standards/publications/rights/index.html for more information.

This article has been accepted for publication in a future issue of this journal, but has not been fully edited. Content may change prior to final publication. Citation information: DOI 10.1109/TASC.2016.2539148, IEEE Transactions on Applied Superconductivity

REFERENCES

[1] O. Kester *et al.*, "Status of the FAIR Accelerator Facility" Proceedings of IPAC2014, pp 2084-2087

[2] S. Aumon, D. Ondreka, S. Sorge, K. Gross, "Transition Energy Crossing in the Future FAIR SIS-100 for Proton Operation, " Proceedings of IPAC2014, pp 1591-1593

[3] J. P. Meier *et al.*, "Development of integrated superconducting quadrupole doublet modules for operation in the SIS100 accelerator," CEC/ICMC 2015 Proceedings

[4] A. M. Baldin *et al.*, "Superconducting fast cycling magnets of the Nuclotron," IEEE Trans. Appl. Supercond. 5, 1995, pp. 875-877

[5] S. Sgobba, G. Hochörtler: "A new non-magnetic stainless steel for very low temperature applications" Proc. International congress STAINLESS STEEL '99 - SCIENCE AND MARKET, Vol. 2, CHIA LAGUNA Sardinia, Italy 6-9 June 1999, pp. 391-401

[6] CERN Accelerator School, "Magnets," 2010, ISBN 978-92-9083-355-0

1051-8223 (c) 2015 IEEE. Personal use is permitted, but republication/redistribution requires IEEE permission. See http://www.ieee.org/publications_standards/publications/rights/index.html for more information.